ADCONIP 2014 Hiroshima

Nonlinear Vibration Control for an Aircraft Vertical Tail by Using Operator-based Estimation

Taiki Nakagawa, Yuta Katsurayama, Mingcong Deng, Shin Wakitani

***Abstract*— In this paper, vibration control is performed by using piezoelectric elements which are one of the smart actuator. An operator-based robust nonlinear control system by using robust right coprime factorization approach and a nonliliner property of hysteresis model is proposed. Considering the hysteresis in the piezoelectric actuator, assuming that an aircraft vertical tail is forced vibration model the response of the plate. Finally, the effectiveness of the proposed nonliner control system is confirmed by simulation results.**

I. Introduction

In recent years, with the use of reinforcing materials such as carbon fiber, the vertical tail becomes light and strong. A tail plays an important role in order to ensure the stability of the yaw direction of the aircraft in the aircraft wing. Generally, it is said that the stability of the aircraft is improved by increasing the area of tail. However, the influence of turbulence and wind is strong. Therefore vibration that occurs the tail becomes increase. This vibration may break the tail and accident of it have occurred in many places. Then, with the development of smart materials, smart material based actuators such as piezoelectric actuators have attracted attention of the researchers. The piezoelectric material has a characteristic that not only can convert mechanical energy into electrical energy, but also can convert electrical energy into mechanical energy. Therefore, they have been used as actuators and sensors. Furthermore, its response is faster and power consumption is small, they are widely used in vibration control. However, a piezoelectric actuator has a nonlinear characteristic that called a hysteresis. So, there is a possibility that the output expected results can not be obtained for input, can not be precise control.

In [1], the distributed ctuator was applied to perform vibration control of cantilever beam. The models of more complex skew plates have also been analyzed in the field of aerospace industry [2]. In [3], the hysteresis property of a piezoelectric actuator was considered and described by using Prandlt-Ishlinskii (PI) model. The vibration control for the plate with piezoelectric actuator was considered in [4]. In this paper, robust nonlinear control method is proposed for suppressing vibration using a piezoelectric element. In [5], setting positions of piezoelectric actuators are selected by using ANSYS. And, in the case of free vibration, the vibration that occures at the tail can be stabilized fast. However, there is a possibility that the vibration is continuously raised forces, such as movement of the body, the air resistance and turbulence to aircraft in the flight.

The Graduate School of Engineering Tokyo University of Agriculture and Technology, 2-24-16 Nakacho, Koganei, Tokyo, 184-8588, Japan

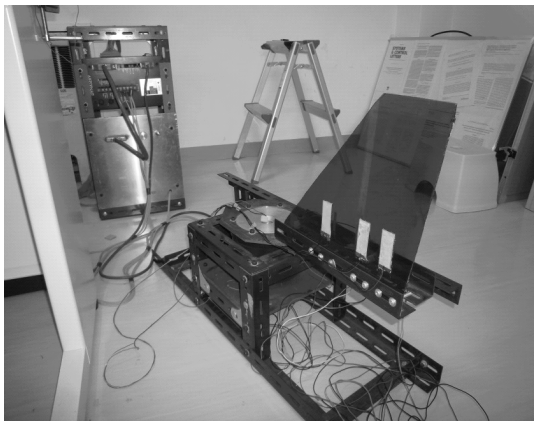

Fig. 1. The experimental system

In this paper, hysteresis property of piezoelectric actuators are considered by using PI model [6]. Setting positions of piezoelectric actuators are selected by ANSYS. Then, the nonlinear control system to the vibration of the plate structure that simulated the aircraft vertical tail is designed by using operator theory [7], [8]. The vibration control simulation of the plate structure are done and the effectiveness of the proposed vibration control method is verified.

The rest of this paper is organized as follows. In section II, experimental devices, model of the external force, the model of aircraft vertical tail, PI hysteresis model and positions of piezoelectric actuators are introduced. The proposed vibration control method is discussed in section III. In section IV, numerical simulation results are shown and verify the effectiveness of the proposed method. In section V, conclusion of this paper is presented.

II. Problem Setup

A. Experimental devices

In this section, experimental devices that are composed in Fig. 1 are introduced. The plate is vibrated by the reciprocating movement of the servo motor. If the piezoelectric sensor that is stuck on the plate structure detects a vibration, it generates an electric charge. In order to process on the PC, that charge is converted to a voltage signal by using a charge amplifier. This signal is transmitted to PCI board that has functions of digital-to-analog and analog-to-digital conversion by passing through the charge amplifier and the inverting amplifier circuit. Then, the control input is calculated by the designed controller. After that, the control input is transmitted to piezoelectric actuators that stick on

the plate by passing through the direct voltage amplifier from PCI board. The output of the direct voltage amplifier is limited between -100 V and +100 V.

B. Model of the external force

Apply force to a plate by reciprocating movement of the servo motor. This session analyses the force applied to the plate. To begin analysing the force, coordinate axes are transformed to the x, y and z-axis of the plate in Fig. 2-b from the ε, ζ and η-axis of it in Fig. 2-a. The coordinate of the micro volume of the plate structure in a certain point (ε, ζ, η) is referred to (1).

$$\begin{aligned}\begin{pmatrix} x' \\ y' \\ z' \end{pmatrix} &= \begin{pmatrix} 1 & 0 & \cos\alpha \\ 0 & 1 & 0 \\ 0 & 0 & \sin\alpha \end{pmatrix} \begin{pmatrix} \eta \\ \zeta \\ \varepsilon \end{pmatrix} \\ \begin{pmatrix} x \\ y \\ z \end{pmatrix} &= \begin{pmatrix} x'+l \\ y' \\ z' \end{pmatrix} \\ &= \begin{pmatrix} \eta+\varepsilon\cos\alpha+l \\ \zeta \\ \varepsilon\sin\alpha \end{pmatrix} \end{aligned} \tag{1}$$

where, the plate structure is on ε, η-axis and l is the distance to the tip of the plate structure from the axis of rotation of the servo motor. Force is given to the plate by rotating the z-axis. When the angular velocity $\vec{\omega}_f(t) = (0, 0, \omega_z(t))$ from the servo motor, the acceleration $\vec{a}(t)$ of the micro volume of the point (x, y, z) is derived as follows:

$$\begin{aligned}\vec{a}(t) &= \frac{d\vec{\omega}(t)}{dt} \times \vec{r} = \begin{vmatrix} \vec{x} & \vec{y} & \vec{z} \\ 0 & 0 & \frac{d\omega_z(t)}{dt} \\ x & y & z \end{vmatrix} \\ &= -\frac{d\omega_z(t)}{dt} y\vec{x} + \frac{d\omega_z(t)}{dt} x\vec{y} \\ &= \frac{d\omega_z(t)}{dt}(\eta + \varepsilon\cos\alpha + l)\vec{y} \end{aligned} \tag{2}$$

where, $\vec{x}$, $\vec{y}$ and $\vec{z}$ represent x, y and z direction, respectively. It is considered to return Fig. 2-a., then (2) is derived as (3).

$$\vec{\gamma}(t) = \frac{d\omega_z(t)}{dt}(\eta + \varepsilon\cos\alpha + l)\vec{\zeta} \tag{3}$$

So, the force that act on the micro volume of the plate structure by reciprocating movement of the servo motor is described as follows:

$$F(t) = \rho t_s \frac{d\omega_z(t)}{dt}(\eta + \varepsilon\cos\alpha + l) \tag{4}$$

C. Model of the plate structure

The controlled object is the plate structure that is simulated the aircraft vertical tail. In Fig. 2-a, $\mathrm{p}_n(n = 1, 2, 3)$ represent piezoelectric actuators and a, b represent length of ε, η direction, respectively. α represents an angle between η-axis and ε-axis. Positions of the actuators are best arranged by using the finite element method. A piezoelectric actuator generates moment, when it is impressed a voltage. This moment is represented as (5) by the Heaviside function $H(\cdot)$. m_ε, m_η represent the magnitude of the moment of the piezoelectric element ε, η direction, respectively.

$$\begin{aligned} m_\varepsilon = m_\eta =& M_p[H(\varepsilon - \varepsilon_{1p_i}) - H(\varepsilon - \varepsilon_{2p_i})] \\ & \cdot [H(\eta - \eta_{1p_i}) - H(\eta - \eta_{2p_i})] \end{aligned} \tag{5}$$

M_p is the moment from piezoelectric actuators ($p = 1, \cdots, 3$). A detail of M_p introduces at section II-D. The equation of motion for the plate structure that is considered piezoelectric actuators is represented as (6). A detail of the external force that applied to the flat plate $F(t)$ was introduced at section II-B.

$$\begin{aligned} D_s\nabla^4\omega + \rho t_s\frac{\partial^2\omega}{\partial t^2} + c_s\frac{\partial\omega}{\partial t} & \\ = \frac{\partial^2 m_\varepsilon(t)}{\partial\varepsilon^2} + \frac{\partial^2 m_\eta(t)}{\partial\eta^2} + F(t) & \end{aligned} \tag{6}$$

where,

$$D_s = \frac{Et_s^3}{12(1-\nu^2)}\ ,\ \nabla^2 = \frac{\partial^2}{\partial\varepsilon^2} + \frac{\partial^2}{\partial\eta^2}$$

ρ, t_s, E, ν and c_s show the density of the tail [kg/m^3], the thickness of the plate [m], an elastic constant [N/m^2], the Poisson's ratio and a damping ratio, respectively. The right side of (6) finds to partial differentiation of (5). The response of the tail is supposed to represent (7).

$$\begin{aligned} \omega(\varepsilon, \eta, t) &= \omega(\varepsilon, \eta)\cdot f(t) \\ &= \sum_{m=1}^{\infty}\sum_{n=1}^{\infty}\phi_m(\varepsilon)\psi_n(\eta)\cdot f(t) \end{aligned} \tag{7}$$

where, $\omega(\varepsilon, \eta)$ is the mode of characteristic vibration. According to the theory of thin plate [9], eigenfunctions $\phi_m(\varepsilon)$ and $\psi_n(\eta)$ are described as follows:

$$\begin{aligned} \phi_m(\varepsilon) =& \cosh\frac{\gamma_\varepsilon}{a}\varepsilon - \cos\frac{\gamma_\varepsilon}{a}\varepsilon - \sinh\frac{\gamma_\varepsilon}{a}\varepsilon + \sin\frac{\gamma_\varepsilon}{a}\varepsilon \\ \psi_1(\eta) =& 1 \\ \psi_2(\eta) =& \sqrt{3}(1 - \frac{2\eta}{b}) \\ \psi_n(\eta) =& \cosh\frac{\gamma_\eta}{b}\eta + \cos\frac{\gamma_\eta}{b}\eta \\ & - \sinh\frac{\gamma_\eta}{b}\eta - \sin\frac{\gamma_\eta}{b}\eta\ ,\ (n > 2) \end{aligned}$$

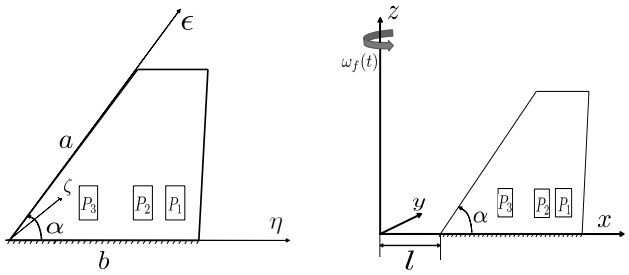

a : The standard coordinate b : The transformed coordinate

Fig. 2. The controlled object

and where $\gamma_\varepsilon = (2m-1)\pi/2$, $\gamma_\eta = (2n-3)\pi/2$. Substitute (7) into (6), $\phi_m(\varepsilon)$ and $\psi_n(\eta)$ satisfy as follows :

$$\int_0^a \phi_m(\varepsilon)\phi_{m1}(\varepsilon)d\varepsilon = \begin{cases} 0, & (m \neq m_1) \\ \int_0^a \phi_m^2(\varepsilon)d\varepsilon, & (m = m_1) \end{cases}$$

$$\int_0^b \psi_n(\eta)\psi_{n1}(\eta)d\eta = \begin{cases} 0, & (n \neq n_1) \\ \int_0^b \psi_n^2(\eta)d\eta, & (n = n_1) \end{cases}$$

from the orthogonality of the natural vibration mode. After multiplying $\phi_m(\varepsilon)\psi_n(\eta)$ at both sides of (6), integrate it in [0, a] , [0, b] and have

$$k_1\frac{d^2f(t)}{dt^2} + k_2\frac{df(t)}{dt} + k_3 f(t) = k_4 M_p(t) + k_5 d(t) \quad (8)$$

where

$$\begin{aligned}
k_1 =& \rho t_s \int_0^a \phi_m^2(\varepsilon)d\varepsilon \int_0^b \psi_n^2(\eta)d\eta \\
k_2 =& c_s \int_0^a \phi_m^2(\varepsilon)d\varepsilon \int_0^b \psi_n^2(\eta)d\eta \\
k_3 =& D_s\left(2\int_0^a \frac{d^2\phi_m(\varepsilon)}{d\varepsilon^2}\phi_m(\varepsilon)d\varepsilon \int_0^b \frac{d^2\psi_n(\eta)}{d\eta^2}\psi_n(\eta)d\eta \right. \\
&+ \int_0^a \frac{d^4\phi_m(\varepsilon)}{d\varepsilon^4}\phi_m(\varepsilon)d\varepsilon \int_0^b \psi_n^2(\eta)d\eta \\
&\left. + \int_0^a \phi_m^2(\varepsilon)d\varepsilon \int_0^b \frac{d^4\psi_n(\eta)}{d\eta^4}\psi_n(\eta)d\eta\right) \\
k_4 =& \left(\frac{d\phi_m(\varepsilon_{2p_i})}{d\varepsilon} - \frac{d\phi_m(\varepsilon_{1p_i})}{d\varepsilon}\right)\int_{\eta_{1p_i}}^{\eta_{2p_i}} \psi_n(\eta)d\eta \\
&+ \left(\frac{d\psi_n(\eta_{2p_i})}{d\eta} - \frac{d\psi_n(\eta_{1p_i})}{d\eta}\right)\int_{\varepsilon_{1p_i}}^{\varepsilon_{2p_i}} \phi_m(\varepsilon)d\varepsilon \\
k_5 =& \rho t_s\left(\int_0^a \phi_m(\varepsilon)d\varepsilon \int_0^b \psi_n(\eta)\eta d\eta \right. \\
&+ \int_0^a \phi_m(\varepsilon)\varepsilon\cos\alpha d\varepsilon \int_0^b \psi_n(\eta)d\eta \\
&\left. + l\int_0^a \phi_m(\varepsilon)d\varepsilon \int_0^b \psi_n(\eta)d\eta\right)
\end{aligned}$$

Then, (7) represents (9) by solving (8).

$$\omega(\varepsilon,\eta,t) = \sum_{m=1}^{\infty}\sum_{n=1}^{\infty}\left[\int_0^t J_{mn}e^{-\alpha_{mn}(t-\tau)}\sin\beta_{mn}(t-\tau) \cdot (k_4 M_p(\tau) + k_5 d(\tau))d\tau\right] \quad (9)$$

where,

$$J_{mn} = \frac{\phi_m(\varepsilon)\psi_n(\eta)}{k_1\sqrt{\frac{k_3}{k_1} - \frac{k_2^2}{4k_1^2}}}$$

$$\alpha_{mn} = \frac{k_2}{2k_1}$$

$$\beta_{mn} = \sqrt{\frac{k_3}{k_1} - \frac{k_2^2}{4k_1^2}}$$

D. Model of the piezoelectric actuator

Prandtl-Ishlinskii hysteresis model based play hysteresis operators is used to describe the moment M_p from the piezoelectric actuator. The play hysteresis operator is defined as [6]:

$$\begin{aligned}
F_h((u)(0);u_1^*) &= f_h((u)(0),u_1^*) \\
F_h((u)(t);u_1^*) &= f_h(u(t),F_h((u)(t_i);u_1^*))
\end{aligned} \quad (10)$$

$$(\ t_i < t \le t_{i+1},\ 0 \le i \le N-1\ )$$

$$f_h(u,q) = \max(u-h,\min(u+h,q)) \quad (11)$$

$$(\ 0 = t_0 < t_1 < \cdots < t_N = t_E, [0,t_E]\ )$$

where $0 = t_0 < t_1 < \cdots < t_N = t_E$ is a partition of $[0,t_E]$ such that the function u is monotone on each of the sub-intervals $[t_i,t_{i+1}]$. $u_1^* \in R$ is an initial value, h is the threshold of the play hysteresis operator.

Here, the play hysteresis operator $F_h(u)(t)$ is given by

$$F_h(u)(t) = \begin{cases} u(t)+h, & u(t) \le F_h(u)(t_i) - h \\ F_h(u)(t_i), & -h < u(t) - F_h(u)(t_i) < h \\ u(t)-h, & u(t) \ge F_h(u)(t_i) + h \end{cases} \quad (12)$$

where $F_h(u)(t)$ is instead of $F_h((u)(t);u_1^*)$ and $F_h((u)(0);u_1^*) = \max(u(0)-h,\min(u(0)+h,u_1^*))$. h is the threshold value of the play hysteresis operator.

Based on the play hysteresis operator, the PI model is represented as [6]:

$$u^*(t) = D_{PI}(u)(t) + \Delta_{PI}(u)(t) \quad (13)$$

where $M_p = u^*$ and parameters of (13) are represented as follows.

$$D_{PI}(u)(t) = Ku(t) \quad (14)$$

$$K = \int_0^{h_x} p(h)dh \quad (15)$$

$$\Delta_{PI}(u)(t) = -\int_0^{h_x} S_n h p(h)dh + \int_{h_x}^{H} p(h)F_h(u)(t_i)dh \quad (16)$$

$$S_n = \text{sign}(u(t) - F_h(u)(t_i)) \quad (17)$$

where h_x is the maximum number that satisfies $h \in [0,h_x]$ and $h \le |u(t) - F_h(u)(t_i)|$ when $h = [h,h_x]$. $p(h)$ is the density function and satisfies (II-D).

$$p(h) \ge 0 \quad , \quad \int_0^{\infty} hp(h)dh < \infty$$

When H exists $h > H$, the density function $p(h)$ satisfies (18).

$$p(h) = 0 \qquad (\ h > H\ ) \quad (18)$$

E. Position of piezoelectric actuator

In this section, optimal setting positions of piezoelectric actuators are shown. In order to select the optimal position, we use finite element method (FEM). FEM is one of the numerical analysis method that obtain an approximate solution of difficult differential equations. Firstly, the object that has a complex form divides simple and optional part. Here, simple and optional parts are called elements. Secondly, differential equations of elements are solved. Then, solutions of differential equation combine, and the whole behaviour is estimated. At this time, we use ANSYS as the software of FEM. ANSYS is the software that can analyse a structure, a vibration, a heat transfer, an electromagnetic field, timbre and a crash at the same time. This time, ANSYS ED 10.0 is used as FEM software. There is a restriction to the number of elements, but it can be used to analyse the displacement of the plate in this time.

The effectiveness of control for a piezoelectric actuator is estimated by (19).

$$g = \frac{\{u\}^T\{u\}}{\{u_0\}^T\{u_0\}} \tag{19}$$

where, $\{u_0\}$, $\{u\}$ and g are the displacement vector of the plate, the displacement vector generated by actuators and the ratio of displacement before and after control, respectively. And considering the voltage of actuators, estimated equations is represented as (20).

$$\Pi = g + Z\frac{\{V\}^T\{V\}}{\{V_0\}^T\{V_0\}} \tag{20}$$

The right second part of (20) is the ratio of the criterial voltage V_0 to the voltage of actuators V_j. Where, V_j is the impressed voltage of the j-th actuator. Z is the parameter considers the effect of control and voltage. If Z becomes large, the effect of the voltage is small. In the opposite side, the effect of the control is large, if Z becomes small. When $Z = 0$, the effect of the control is maximum. Here, if the parameter of Π is minimum, there is the most effective position of the piezoelectric actuator to control the vibration. The position of actuators are chosen in this way by using ANSYS.

III. The proposed design scheme

In this section, a design of the nonlinear system with hysteresis is proposed by using robust right coprime factorization condition. The framework of the considered system is shown in Fig. 3. $r \in Y$, $e_1 \in Y$ are the input of the controller C_{PI}, $e_2 \in U$ is the input of the controller B^{-1}, $b \in U$ is the output of the controller A, d^* is external force, $u \in U$ and $u^* \in U^*$ are the input of PI model and input of the nonlinear plant, respectively. Where, U is the input space of the PI model, and U^* is the output spaces of the PI model. Let output space of original nonlinear plant and quasi-state space be Y and W, respectively. Then a detail of Δ_{dis} is introduced at section III-C.

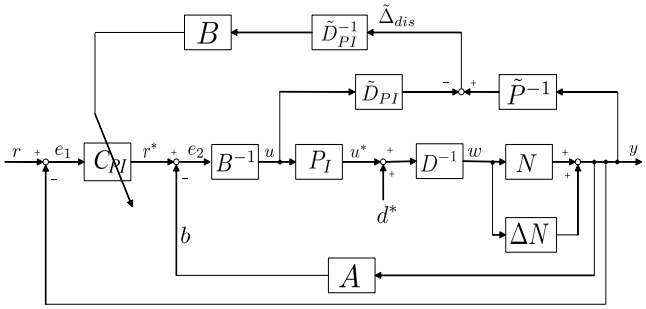

Fig. 3. The proposed control system

A. Right factorization of the model

All of the control objects are expressed at time domain and designed controller based on operator theory [7]. The model of the control object is expressed (9).

In this paper, we consider the nominal vibration mode with a first and the uncertainty with second and third order modes. So the plant is considered the following equation.

$$\begin{aligned}[P+\Delta P]((u^*)(t)+(d^*)(t)) &= (1+\Delta)\left[J_{11}\int_0^t e^{-\alpha_{11}(t-\tau)}\sin\beta_{11}(t-\tau)\right.\\ &\qquad \left.\cdot(u^*(\tau)+d^*(\tau))d\tau\right] \end{aligned} \tag{21}$$

Plant $P+\Delta P$ is factorized following equations.

$$\begin{aligned} P+\Delta P &= (N+\Delta N)D^{-1}((u^*)(t)+(d^*)(t)) \\ &= (N+\Delta N)D^{-1}(P_I(u)(t)+d^*(t)) \end{aligned} \tag{22}$$

$$[N+\Delta N](w)(t) = (1+\Delta)\cdot\left[J_{11}\int_0^t e^{-\alpha_{11}(t-\tau)}\sin\beta_{11}(t-\tau)\cdot w(\tau)d\tau\right] \tag{23}$$

$$D(w)(t) = I(w)(t) \tag{24}$$

where $I(\cdot)$ is the identity operator.

B. Controller design of a stability

Consider the nonlinear plant $\tilde{D} = D_{PI}^{-1}D$, and Δ_{PI} is bounded uncertainty. In this case, the output of the plant $y(t)$ is represented following equation.

$$\begin{aligned} y(t) = &(N+\Delta N)(A(N+\Delta N)+B\tilde{D})^{-1} \\ &\cdot(r^*(t)+BD_{PI}^{-1}(\Delta_{PI}+d^*)) \end{aligned} \tag{25}$$

The controller A and B are decided to satisfy bezout identity (26).

$$AN + B\tilde{D} = M \tag{26}$$

$$A(y)(t) = \left(\frac{1-K_m}{J_{11}\beta_{11}}\right)\left(\ddot{y}+2\alpha_{11}\dot{y}+(\alpha_{11}^2+\beta_{11}^2)y\right) \tag{27}$$

$$B(u)(t) = K_m K u(t) \tag{28}$$

where K_m, M are design parameter and unimodular operator, respectively. And, K is represented by (29).

$$K = \int_0^{h_x} p(h)dh \tag{29}$$

In the simulation, the uncertainty Δ is known and considered second and third mode of the tail's vibration. Then, robust stability is represented as following equation.

$$\|[A(N+\Delta N)-AN]M^{-1}\|_{Lip} < 1 \tag{30}$$

C. Design of a controller on vibration compensator

The stability of the system is guaranteed by designing controllers A and B. However, if there are controllers A and B, the output $y(t)$ will not track the target value $r(t)$.

$$y(t) = (N+\Delta N)\tilde{M}^{-1}(r^*(t) + BD_{PI}^{-1}\Delta_{dis}) \tag{31}$$

$$\Delta_{dis} = (\Delta_{PI} + d^*(t)) \tag{32}$$

From (32), the tracking controller C_{PI} is designed as follow:

$$C_{PI}(e_1)(t) = k_p e_1(t) + k_I \int_0^t e_1(\tau)d\tau - BD_{PI}^{-1}\tilde{\Delta}_{dis} \tag{33}$$

where k_p, k_I are design parameters. $\tilde{\Delta}_{dis}$ is the value that estimated Δ_{dis}. $\tilde{\Delta}_{dis}$ is calculated using estimated mechanism shown in Fig. 3.

$$\begin{aligned}\tilde{P}^{-1}(y)(t) &= (P+\Delta P)^{-1}(y)(t) \\ &= \tilde{D}_{PI}(u)(t) + \tilde{\Delta}_{PI} + \tilde{d}^*(t) = \tilde{u}^*(t)\end{aligned} \tag{34}$$

$\tilde{\Delta}_{dis}$ is estimated by taking the differences between calculation results of $\tilde{u}^*(t)$ and $\tilde{D}_{PI}(u)(t)$. Where, $\tilde{D}_{PI}$ is computable. C_{PI} performs disturbance rejection and improved tracking performance. So, the tracking performance of the system is guaranteed to satisfy (35).

$$y(t) = (N+\Delta N)\tilde{M}^{-1}(C_{PI} + BD_{PI}^{-1}\Delta_{dis}) \tag{35}$$

The control system that is represented as (35) is the same system of [3] and [4]. In [3] and [4], output of the system was confirmed to track $r(t)$. So, the system represented as (35) tracks $r(t)$.

IV. Simulation results

In this section, simulation results are shown by using designed controllers.

A. Parameter setting

Simulation results show the vibration control performance of the tail. Parameters of the plate structure and piezoelectric actuators are shown in Table I and II, respectively.

TABLE I
PARAMETERS OF THE PLATE STRUCTURE

Young's modulus	E	=	2.94×10^9	N/m^2
Poisson's ratio	ν	=	0.38	–
Density	ρ	=	1430	kg/m^3
Length of ε direction	a_p	=	0.31	m
Length of η direction	b_p	=	0.27	m
Thickness	t_s	=	2×10^{-3}	m
Bending stiffness	D_s	=	$E\cdot\frac{t_s^3}{12(1-\nu^2)}$	N·m
Damping ratio	c_s	=	0.6	–

In simulations, the vibration on ε direction is just considered. On η direction, the only first order mode of aircraft vertical tail is used. And the first mode order of the tail is considered on ε direction, and second and third order modes of it are contained as uncertainties ΔP. So, we choose $m=3$ and $n=1$ to describe the considered aircraft vertical tail. And use density function of piezoelectric elements $p(h) = 0.00032\times e^{-0.00086(h-1)^2}$ where $h\in[0,100]$.

TABLE II
PARAMETERS OF PIEZOELECTRIC ACTUATORS

Young's modulus	E^p	=	6.2×10^{10}	N/m^2
Length	a	=	50×10^{-3}	m
Width	b	=	20×10^{-3}	m
Thickness	t_p	=	0.5×10^{-3}	m
Piezoelectric constant	d_{31}	=	-210×10^{-12}	m/V

TABLE III
PARAMETERS OF SIMULATION

designed parameter	k_p	=	0.65
	k_I	=	0.15
	K_m	=	0.98
sampling time	0.01		s
simulation time	60		s

B. Simulation results

In this simulation, the servo motor is reciprocated at an angular velocity $\omega_f(t) = 0.0085\sin(2\pi f_{dis}\cdot t)$ [rad/s] as a periodic external force, f_{dis} is assumed that the eigenfrequency $f_{dis} = 5.21$ Hz of the plate structure. Start to control of forced vibration 5 sec later after adding the vibration. If the nominal plant defined a first order mode of the vibration, Δ is considered as second and third order modes of it. Parameters of simulation is shown in Table III. The simulation results of vibration control for the plate structure are shown in following figures. In Fig. 4, the simulation result without control shows a dashed line. At the full line in Fig. 4, we show the result of simulation using the controller A and B that designed in section III without the tracking controller C_{PI}. The condition of robust stability is represented at (30). Robust stability is shown in Fig. 5. In Fig. 5, condition of robust stability is less than 1, so the proposed system can be confirmed robust stable. Furthermore, making the improvement of the damping performance by using the tracking controller C_{PI} in Fig. 6. The corresponding control input of piezoelectric actuators are shown in Fig. 7.

Fig. 8 is the output of the system with and without the tracking controller C_{PI}. In Fig. 8, the simulation result without the tracking controller C_{PI} shows a outside line. At the inside line in Fig. 8, the simulation result with C_{PI}.

C. Consideration

Fig. 8, good damping performance was shown by using the tracking controller C_{PI}. In results, it is understood that the control system is stabilized by using the designed controllers A and B in section III and that control on vibration performance is good by using the tracking controller C_{PI}.

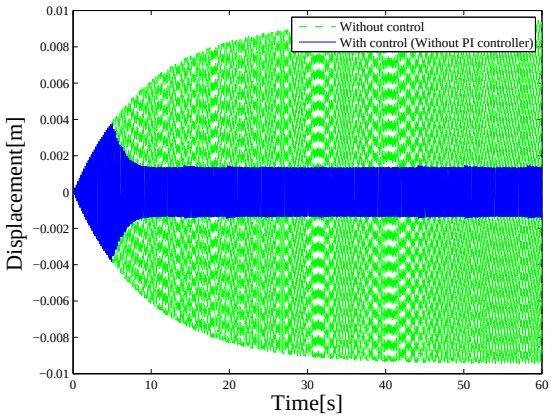

Fig. 4. The output of the system without the tracking controller C_{PI}

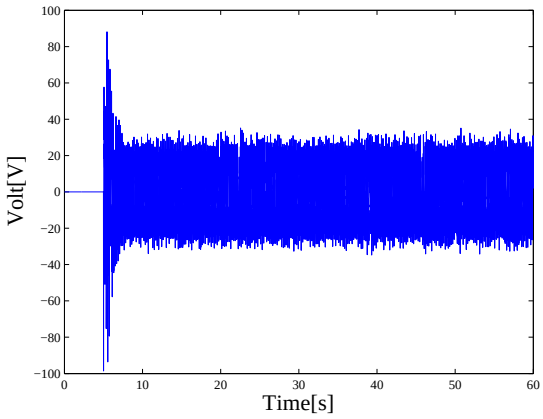

Fig. 7. Control input of piezoelectric actuators

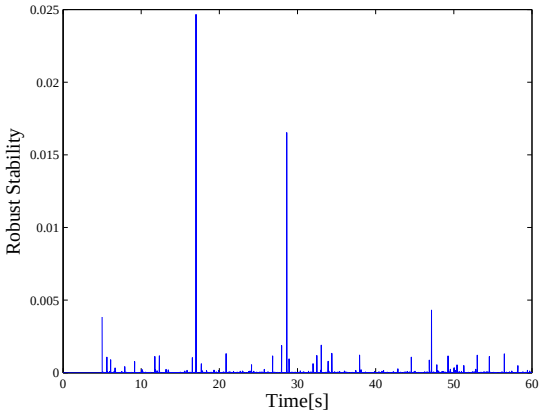

Fig. 5. Robust stability

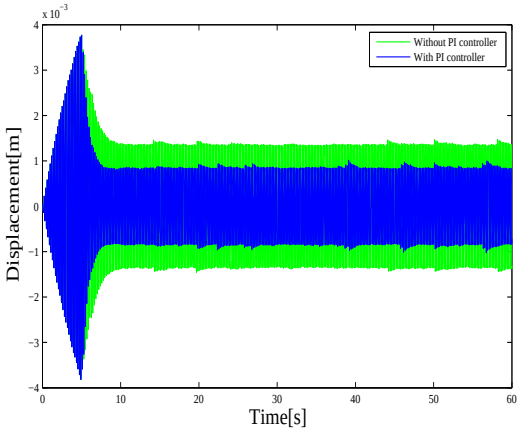

Fig. 8. The output with and without the tracking controller C_{PI}

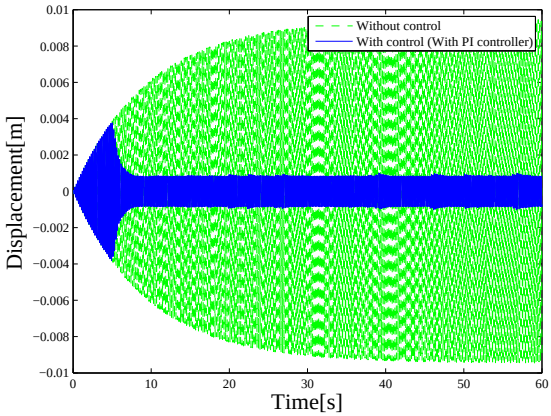

Fig. 6. The output of the system with the tracking controller C_{PI}

V. Conclusion

In this paper, the model of the vibration of the plate structure and the piezoelectric actuator are constructed. In order to control the vibration of the plate structure by using piezoelectric actuators, control design method based on an operator theory was proposed. And periodic external force was applied to the plate structure, the effectiveness of the proposed method was verified by simulation of the forced vibration. Therefore, it was confirmed to realized desired vibration control performance.

References

[1] T. Bailey and J. E. Hubbart, Distributed piezoelectric-polymer active vibration control of a cantilever beam, *Jounal of Guidance,Control and Dynamics*, vol. 8, no. 5, pp. 605-611, 1985.

[2] M. K. Singha and R. Daripa, Nonlinear vibration of symmetrically laminated composite skew plates by finite element method, *International Jounal of Non-linear Mechanics*, vol. 42, no. 9, pp. 1144-1152, 2007.

[3] S. Saito, M. Deng, A. Inoue, and C. Jiang, Vibration control of a flexible arm experimental system with hysteresis of piezoelectric actuator, *International Journal of Innovative Computing, Information and Control*, Vol. 6, No. 7, pp. 2965-2975, 2010.

[4] C. Jiang, M. Deng, and T. Tomono, Operator-based Vibration Control for Aircraft Vertical Tail with Piezoelectric Actuator, *Proceedings of the 2010 IEEE Multi-Conference on Systems and Control*, pp. 2397-2402, 2010.

[5] Y. Katsurayama, C. Jiang, and M. Deng, Experimented Study of Nonlinear Vibration Control for Vertical Tail with Considering Low order Mode, *Proceedings of the ICAMechS 2013*, pp.335-340, 2013.

[6] M. Deng, C. Jiang, A. Inoue, and C. Y. Su, Operator based robust control for nonlinear systems with Prandtl-Ishlinskii hysteresis, *International Journal of Systems Science*, Vol.42, No.4, pp. 643-652, 2011.

[7] M. Deng, A. Inoue, and K. Ishikawa, Operator based nonlinear feedback control design using robust right coprime factorization, *IEEE Transactions on Automatic Control*, Vol. 51, No. 4, pp. 645-648, 2006.

[8] M. Deng, Operator-Based Nonlinear Control Systems Design and Applications (IEEE Press Series on Systems Science and Engineering), Wiley-IEEE Press, 2014.

[9] A. W. Leissa, Vibration of plates, *Acoustical Society of Amer*, 1993.